Beam Size Measurements using Coded Apertures at Low-Emittance Rings

John Flanagan

Topical Workshop on Emittance Measurements for Light Sources and FELs

Barcelona

2018.1.29

Outline

- Principles of Coded Aperture Imaging
- Experiences so far at:
  - Diamond Light Source
  - CesrTA
  - SuperKEKB
- Summary and Prospects

Principles of Coded Aperture Imaging

- Technique developed by x-ray astronomers using a mask to modulate incoming light. Resulting image must be deconvolved through mask response (including diffraction and spectral width) to reconstruct object.
- Idea proposed by x-ray astronomer R. Dicke to use multiple pinholes to increase photon-collection efficiency.
  - He proposed randomly-spaced pinholes.
  - Produces complicated detector image, that can be recovered by deconvolution by cross-correlation with original mask image.

R.H. Dicke, Astrophys. Journ., 153, L101, (1968).

Principles of Coded Aperture Imaging

- In principle, any set of multiple apertures can be considered a “coded aperture.”
  - Even Fresnel zone plates have been proposed for used as coded apertures – if detuned so as not to act like lens, then it provides a uniformly spaced set of aperture widths and spacings, for uniform spatial resolution over a range of sizes.
- Special case: Uniformly Redundant Arrays (URAs)
  - Pseudo-random arrangement of apertures, with nice mathematical property that auto-correlation is a delta function, so reconstruction has no side-lobe artifacts, as tend to occur for truly random arrays (and FZPs).

E.E. Fenimore and T.M. Cannon, Appl. Optics, V17, No. 3, p. 337 (1978).

Principles of Coded Aperture Imaging

- In practice, due to issues of dealing with background and detector noise, most practical applications of coded aperture imaging for x-ray astronomy have been based on iterative methods, rather than direct deconvolution.
  - Modify proposed source distribution until it generates similar image to measured detector image.
  - In astronomy, one does not know what the source distribution should look like, and it is important not to create spurious sources through reconstruction artifacts.
- For accelerator-based measurements, we have the additional issues due to not operating in classical limit, which direct deconvolution method assumes.
  - Diffraction effects
  - Spectral response of detector, and variation of spectrum on- and off-axis
  - Non-uniform intensity profile of incident beam, unlike what can be assumed for astronomical sources.
- For accelerator beam measurement, we have thus far made use of template fitting:
  - Create an array of simulated detector images for different beam sizes and position offsets, and fit measured detector image against these templates to find the closest match.
  - Very brute-force, but with multi-cpu reconstruction machines, we can keep up with measurement rates of a few Hz.
  - Works because we generally know that the source distribution should look like: usually a single gaussian of unknown size and position, to be determined.

Why URA mask?

- Advantage over simple pinhole/slit:
  - Greater open aperture for single-shot measurements
    - Also useful for low-current studies
      - At SuperKEKB, optics tuning is done at low currents to protect the detector from beam-loss backgrounds, before ramping back up to full currents for collision data-taking.
      - Optics group needs beam sizes at low currents to evaluate tuning effectiveness.
  - Somewhat better resolution
    - Get some peak-valley ratios that help at smaller beam sizes.
    - Make use of more of the detector, improve S/N
- What about a simple equal-spaced array of pinholes/slits?
  - Flatter spatial frequency response
    - Better chance of reconstructing shape
    - Unique position determination (non-repeating pattern)
  - On the other hand, an equal-spaced array can offer tuned resolution over a narrower range of sizes
    - Array may be suitable for a very stable machine, such as a light source.
- For instability studies (e-cloud, e.g.) or other machine studies, or for a luminosity machine which is always running at the limit of stability, a URA mask promises better performance over a range of bunch conditions.

What the detector sees

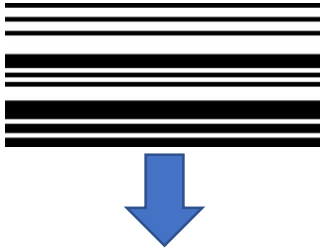

- Source SR wavefront amplitudes:

$$\begin{bmatrix} A_\sigma \\ A_\pi \end{bmatrix} = \frac{\sqrt{3}}{2\pi}\gamma\frac{\omega}{\omega_c}\left(1+X^2\right)(-i)\begin{bmatrix} K_{2/3}(\eta) \\ \frac{iX}{\sqrt{1+X^2}}K_{1/3}(\eta) \end{bmatrix},$$

where

$$X = \gamma\psi,$$

$$\eta = \frac{1}{2}\frac{\omega}{\omega_c}\left(1+X^2\right)^{3/2},$$

K.J. Kim, AIP Conf. Proc. 184 (1989).

J.D. Jackson, "Classical Electrodynamics," (Second Edition),John Wiley & Sons, New York (1975).

- Kirchhoff integral over mask (+ detector response)
  → Detected pattern:

$$A_{\sigma,\pi}(Detector) = \frac{iA_{\sigma,\pi}(Source)}{\lambda}\times \int_{mask}\frac{t(y_m)}{r_1 r_2}e^{i\frac{2\pi}{\lambda}(r_1+r_2)}\left(\frac{\cos\theta_1+\cos\theta_2}{2}\right)dy_m$$

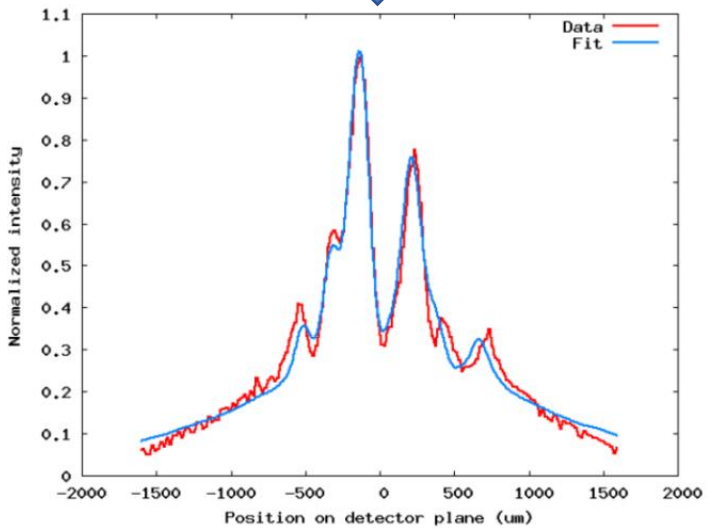

Measured slow-scan detector image (red) at CesrTA, used to validate simulation (blue)

- $t(y_m)$ is complex transmission of mask element at y_m.
- Sum intensities of each polarization and wavelength component.
- Sum weighted set of detector images from point sources.
  - The source beam is considered to be a vertical distribution of point sources.
  - Can also be applied to sources with non-zero angular dispersion and longitudinal extent, for more accurate simulation of emittance and source-depth effects.
  - For machines under consideration here these effects are small, so for computational speed we restrict ourselves to 1-D vertical distributions.

Introduction: Target machines

X-ray Source Parameters:

Parameter	CesrTA (low-energy)	Diamond Light Source	SuperKEKB Low Energy Ring / High Energy Ring
ε_y (pm-rad) (minimum)	<20	~8	~10
σ_y (μm) (minimum) (at x-ray source point)	~10	~7	~10
Beam Energy (GeV)	2.085	3	4 / 7
Bending radius (m)	31.65	7.15	31.74 / 106
Critical Energy (keV)	0.64	8.4	4.5 / 7.2

Machines:

- CesrTA
  - ILC damping ring and low-emittance ring test machine, with focus on low-emittance tuning and electron-cloud studies.
- Diamond Light Source
- SuperKEKB
  - Super B factory: e+ e- two-ring energy-asymmetric collider for new physics searches.

Experience at Diamond LS

Beamline, detector:

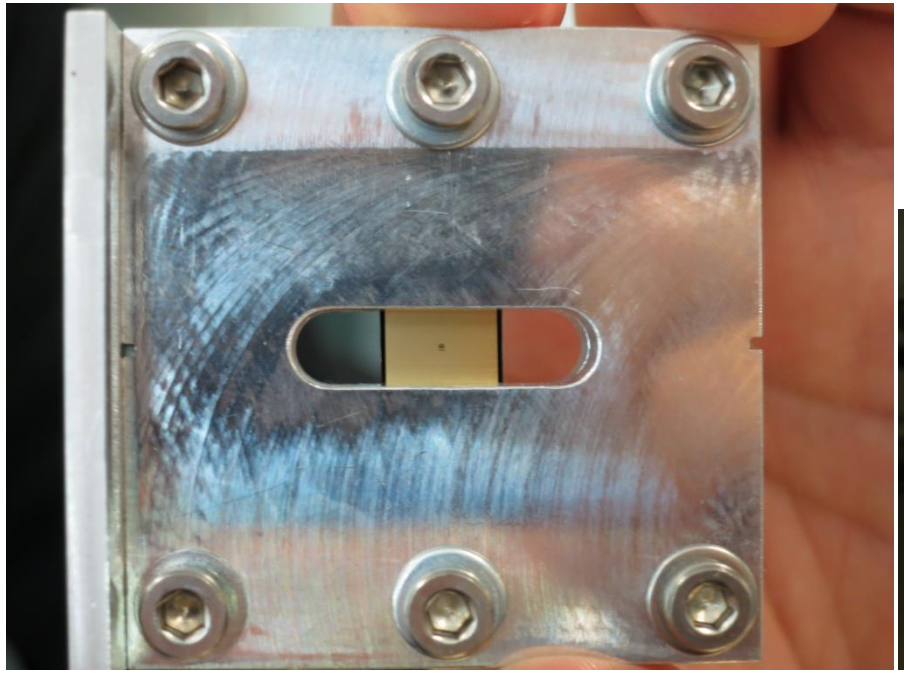

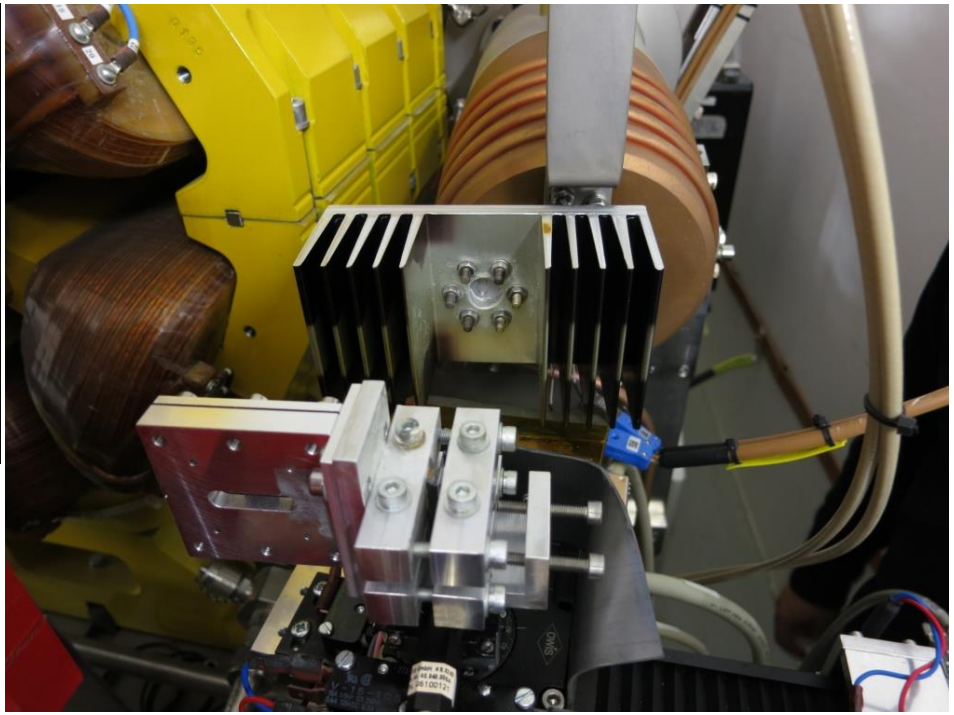

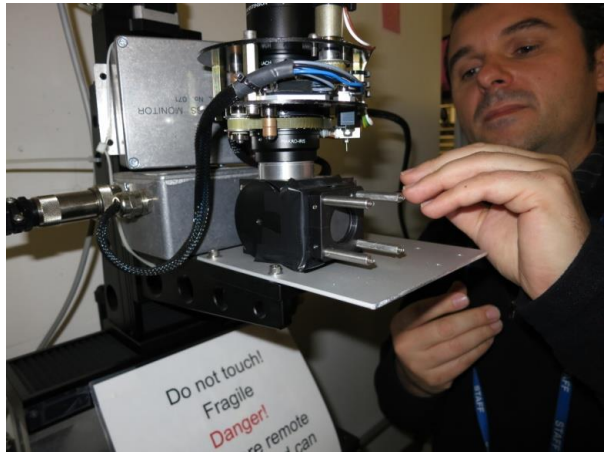

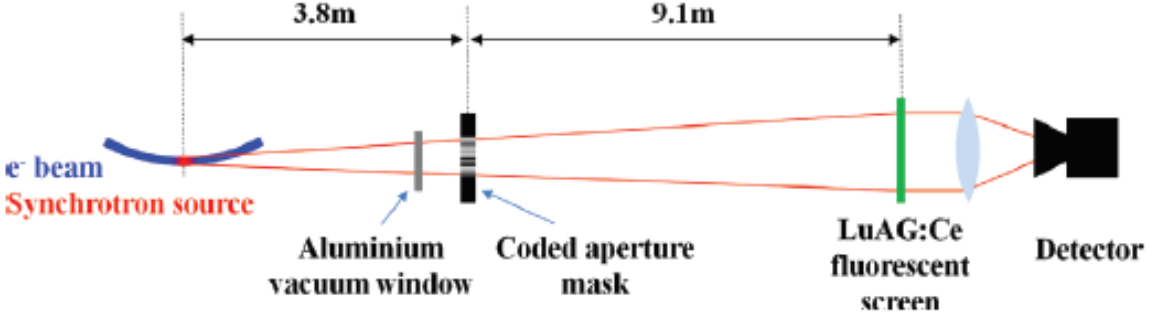

Figure 3: Basic schematic layout of the coded aperture beamline.

Experience at Diamond LS

Measurement results:

- Using spare high-energy optic (Au+Si) designed for SuperKEKB:
  - 10 μm x 59 URA
  - 18.2 μm Au mask on 625 μm Si substrate
- Detector:
  - 200 μm LuAG:Ce screen
  - 1024(H)x768(V) pixel camera
- **Not single-shot measurements, but sufficiently detailed data to demonstrate validity of fitting model.**

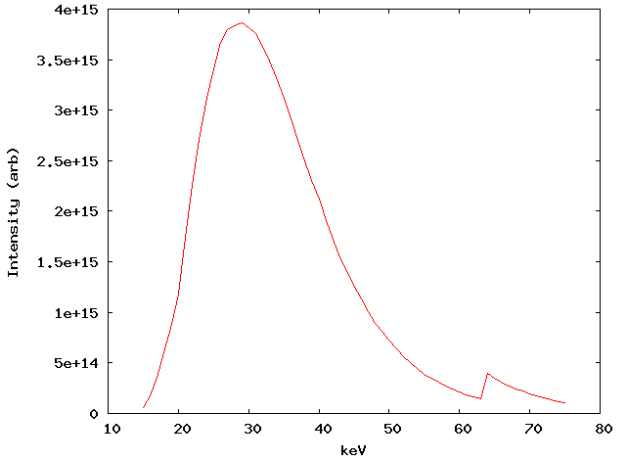

Modeled detected spectrum

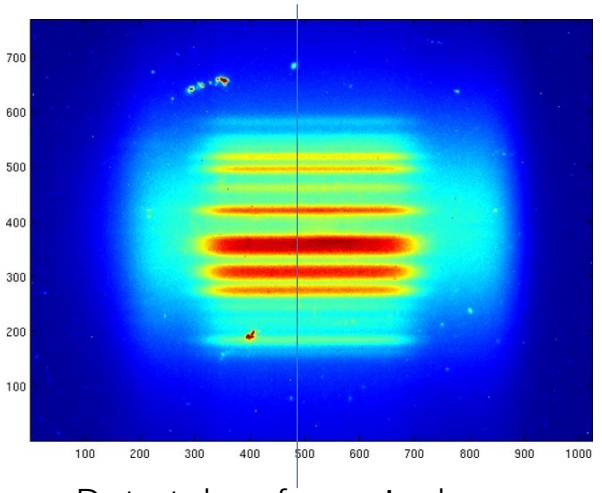

Data taken from single-pixel-width line near center

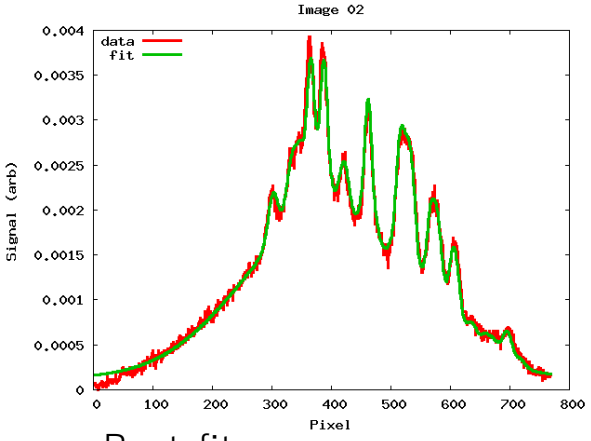

Best-fit:
--Beam size: 10.5 μm
--Mask position relative to beam: 166 μm

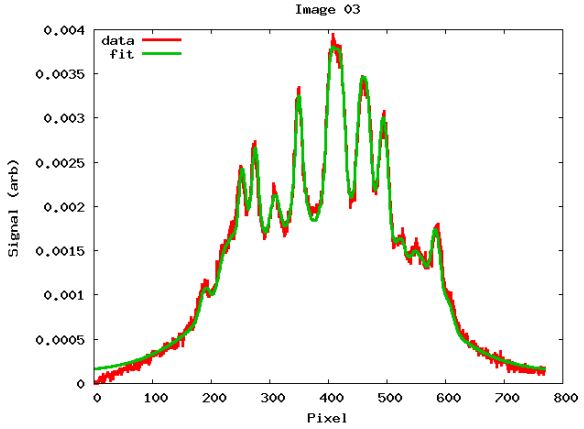

Best-fit:
--Beam size: 10.4 μm
--Mask position relative to beam: 5 μm

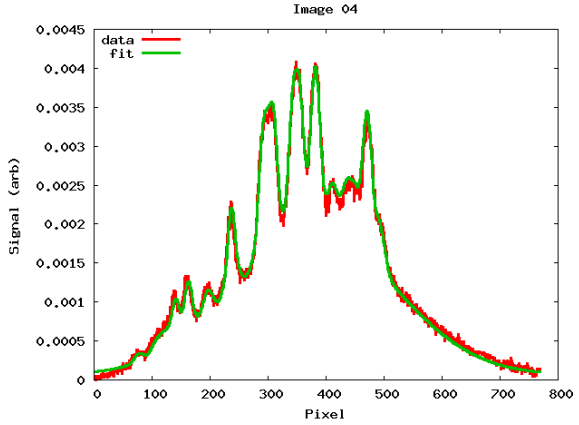

Best-fit:
--Beam size: 10.6 μm
--Mask position relative to beam: -126 μm

Experience at Diamond LS

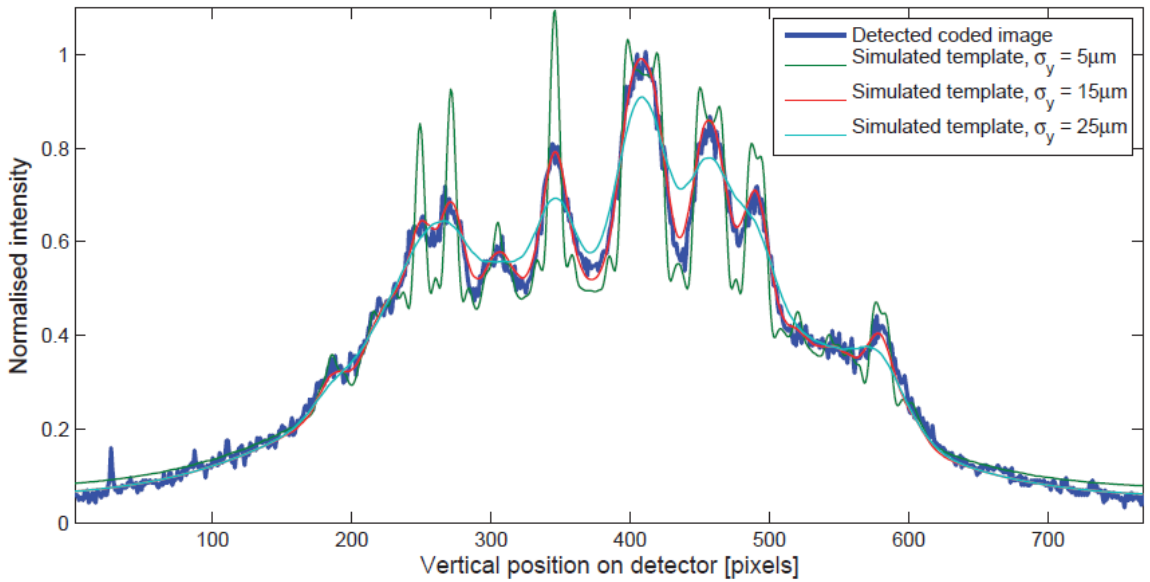

Figure 6: The detected flux for nominal beam conditions (~0.3 % coupling, κ) as seen by a single column of pixels from the camera, plotted along with the generated templates for flux seen at each detector pixel for three different vertical source sizes, σ_y.

The coded aperture measurements of vertical electron beam size correlate well with those measured by the existing pinhole cameras at DLS, although unexplained differences in the measured beam size are observed. The coded aperture measurements consistently give a smaller beam size than that found using the pinhole camera. Resolution of the coded aperture system is found to be on par with that obtained with the pinhole cameras, although the clear discrepancies between the measurements of the two systems require further investigation.

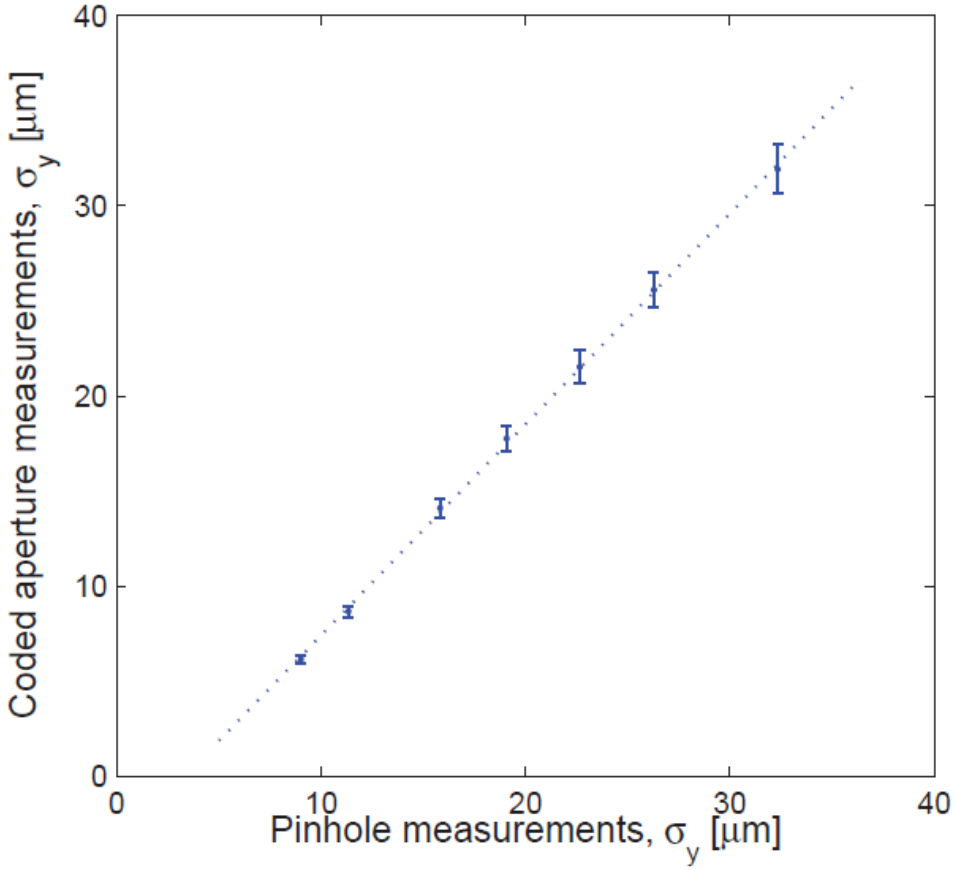

Figure 7: A plot comparing the vertical electron beam size measurements calculated from pinhole images, and calculated from from coded aperture images. A best fit line is shown.

C. Bloomer, G. Rehm, J.W. Flanagan, "MEASUREMENTS OF SMALL VERTICAL BEAMSIZE USING A CODED APERTURE AT DIAMOND LIGHT SOURCE,"
Proceedings of IBIC2014, Monterey, CA, USA, p. 279 (2014)

Experience at CesrTA

D Line x-ray beam line

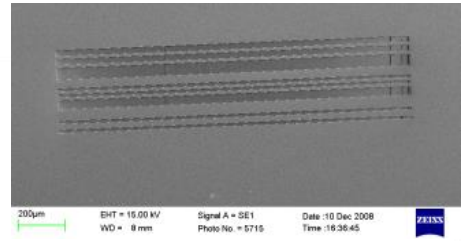

CA mask
(Applied Nanotools)
0.5 μm Au mask
2.5 μ Si substrate

Diamond window

Detector box

Screens, slits etc. for alignment

Optics box
(CA, FZP, slit)

Source bend (not shown)

CesrTA: Data Analysis

- 1) Simulate point response functions (PRFs) from various source positions to detector, taking into account beam spectrum, attenuations and phase shifts of mask and beamline materials, and detector response.
- 2) Add PRFs, weighted to possible proposed beam distributions.
- 3) Find best fit to detector data.

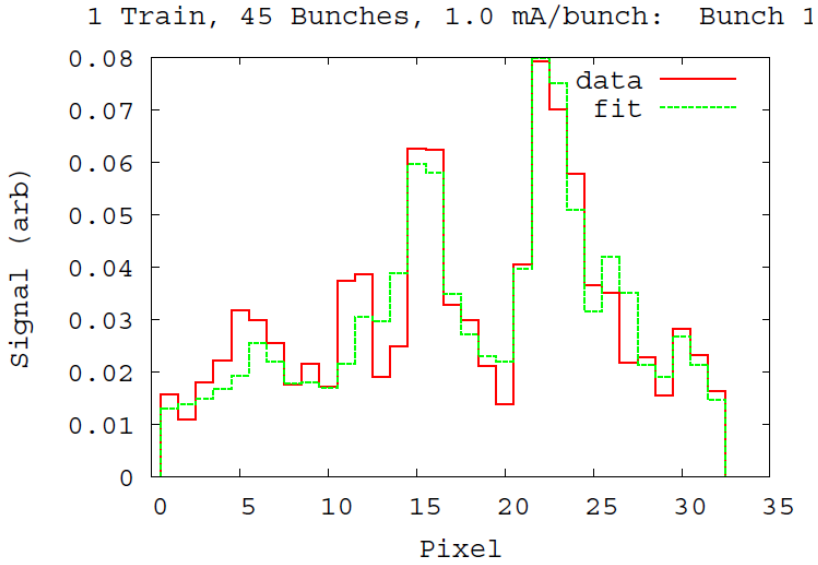

Example of single-shot data (single-bunch, single-turn)

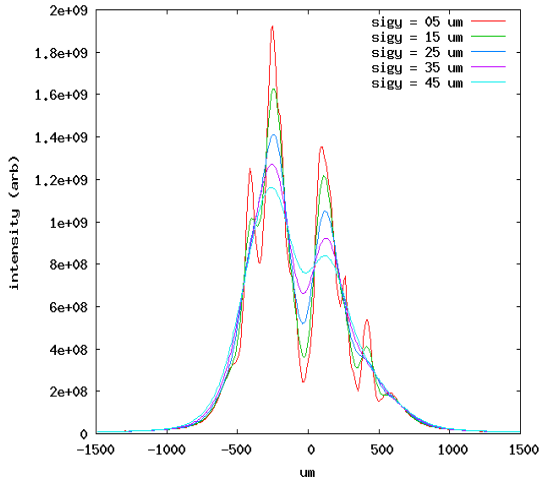

Simulated detector image for various beam sizes at CesrTA

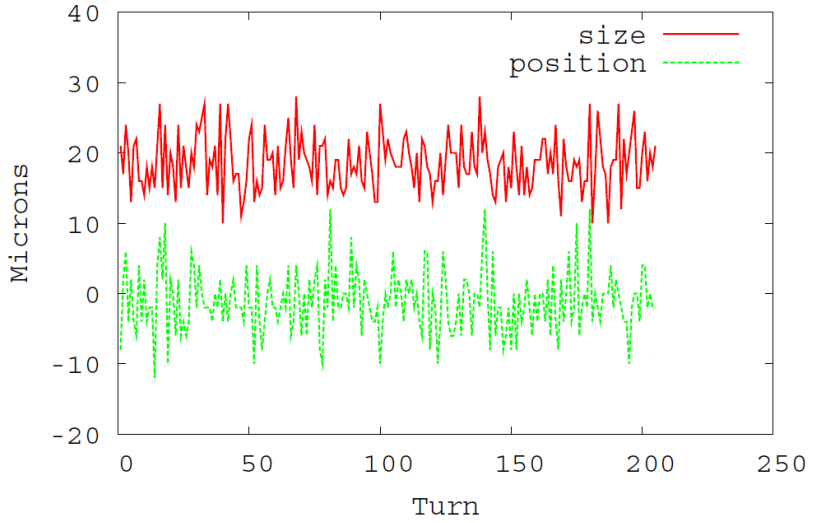

Example of turn-by-turn data (one bunch out of train)

CesrTA: Electron-cloud study data

- Study of effect of electron clouds on beam size.
- As cloud density increases along train, size of bunch increases due to presence of clouds.
- We can use this range of sizes to compare with resolution estimates.
  - Compare spread of sizes at each bunch with calculated resolution confidence intervals.

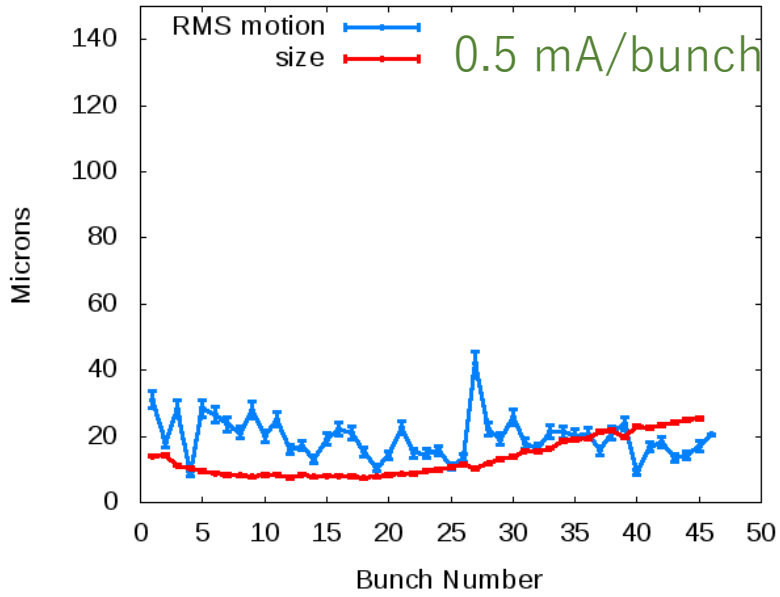

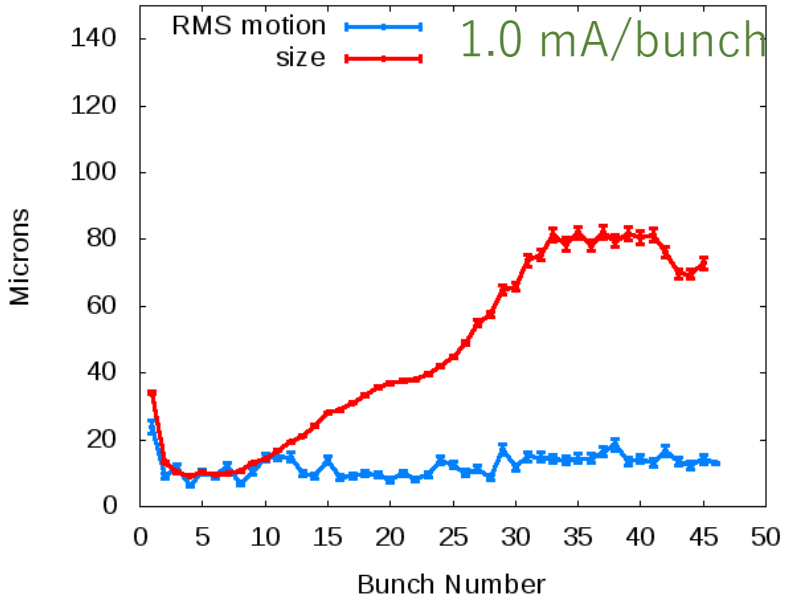

Single-shot resolution estimation

- Want to know, what is chance that a beam of a certain size is misfit as one of a different size?
- Tend to be photon statistics limited. (Thus coded aperture.)
- So:
  - Calculate simulated detector images for beams of different sizes
  - "Fit" images pairwise against each other:
    - One image represents true beam size, one the measured beam size
    - Calculate χ^2/ν residuals differences between images:

N = # pixels/channels
n = # fit parameters (=1, normalization)
S_i = expected number of photons in channel i

$$\frac{\chi^2}{\upsilon} = \frac{1}{N-n-1}\sum_{i=1}^{N}\frac{[s_i' - s_i]^2}{\sigma_i^2},$$

    - Weighting function for channel i: $\sigma_i = \sqrt{s_i}\,.$
  - Value of χ^2/ν that corresponds to a confidence interval of 68% is chosen to represent the 1-s confidence interval

10 μm, 31-element CA mask @ D Line 2 GeV

Generate detector images for various beam sizes:

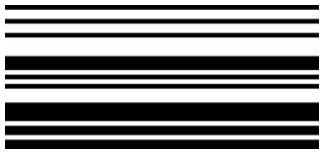

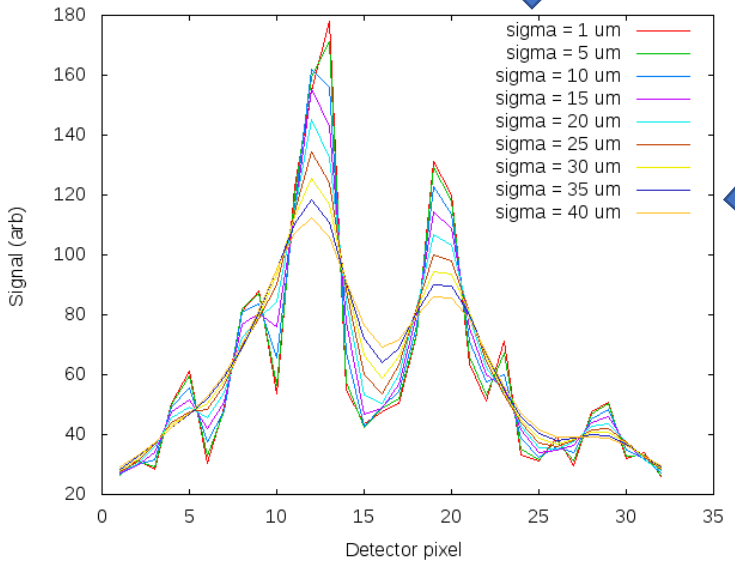

Cross-fit between beam sizes.
Plot 1-sigma statistical confidence regions,
Assuming 200 photons/pixel average
(=> 0.56 mA at 2 GeV):

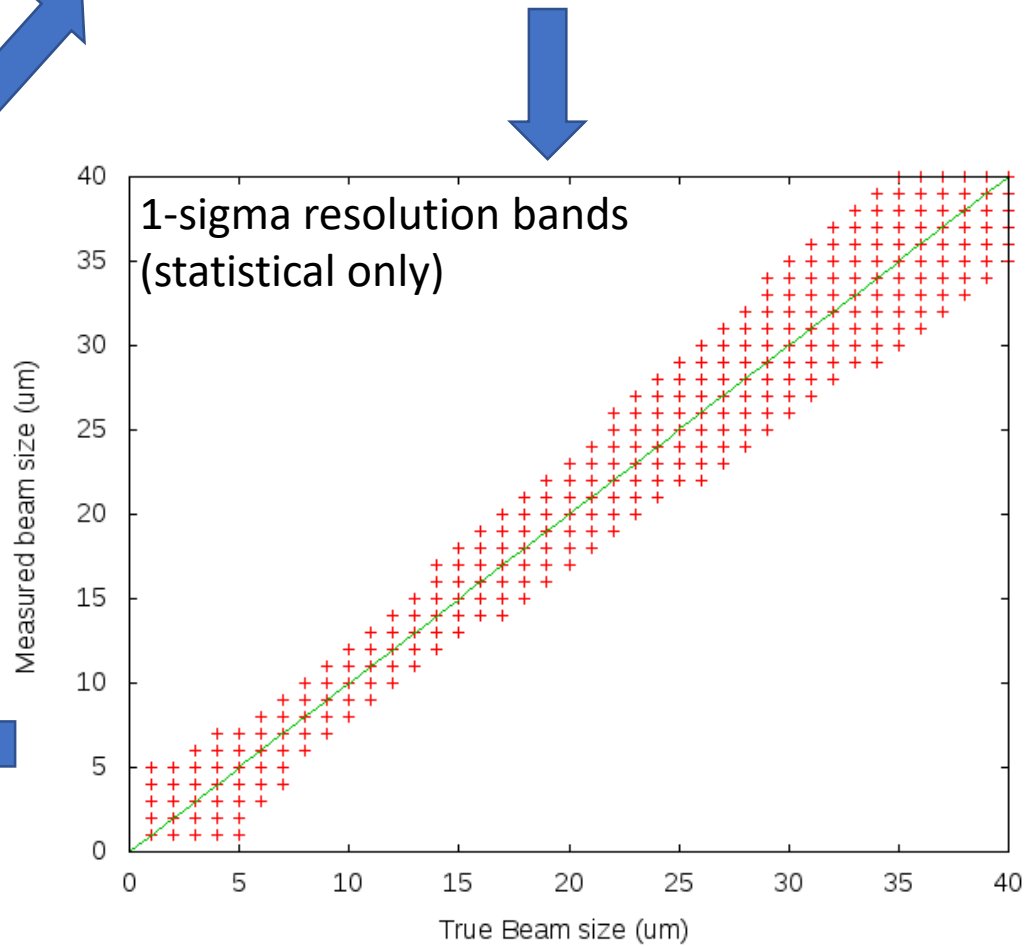

Statistical single-shot resolution at 10 μm beam size = +/- ~2 μm
(Assuming ideal detector.)

CesrTA: Resolution data vs simulation with CA

- Using May 10 2010 E-Cloud study data as data source.
- Simulation statistical confidence bands assume
  - Perfect, noiseless detector
  - 200 photons/pixel/shot on average
    - =>0.56 mA/bunch
- Shot-by-shot spread in data is between that at 0.5 mA and 1.0 mA in the data
  - Not using a perfect, noiseless detector.

- Reasonable agreement

- For more detailed evaluation, including effects of detector noise, see below:

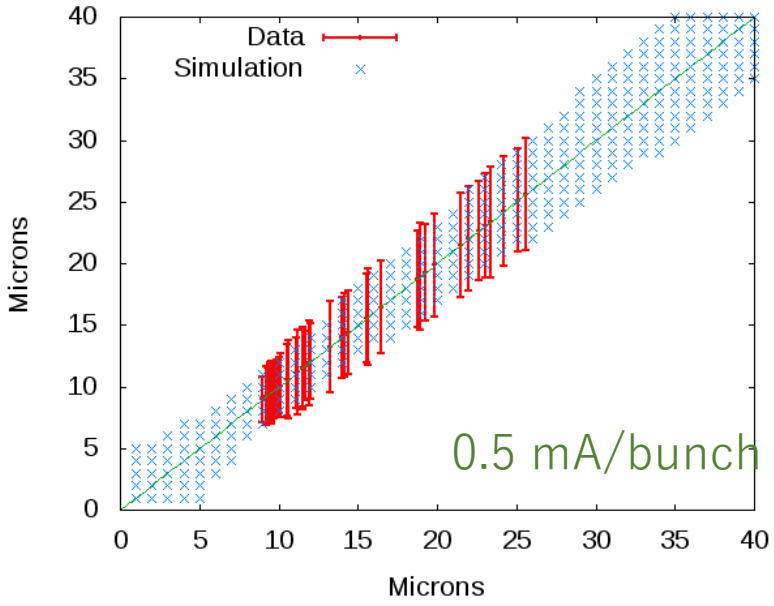

1 Train, 45 Bunches, 1 mA/bunch

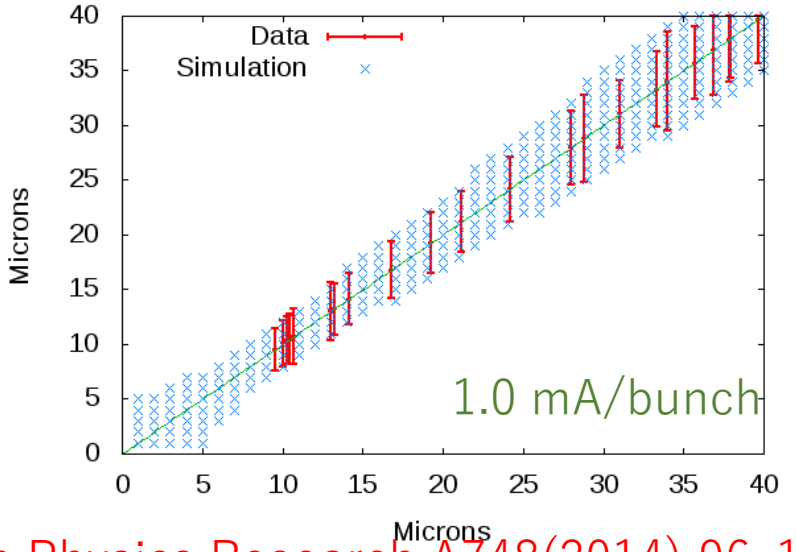

J.P. Alexander et al., Nuclear Instrumentsand Methods in Physics Research A748(2014) 96–125

CesrTA Alternate CA: Make use of interference peaks

URA

Enhanced diffraction peak design (Dan Peterson)

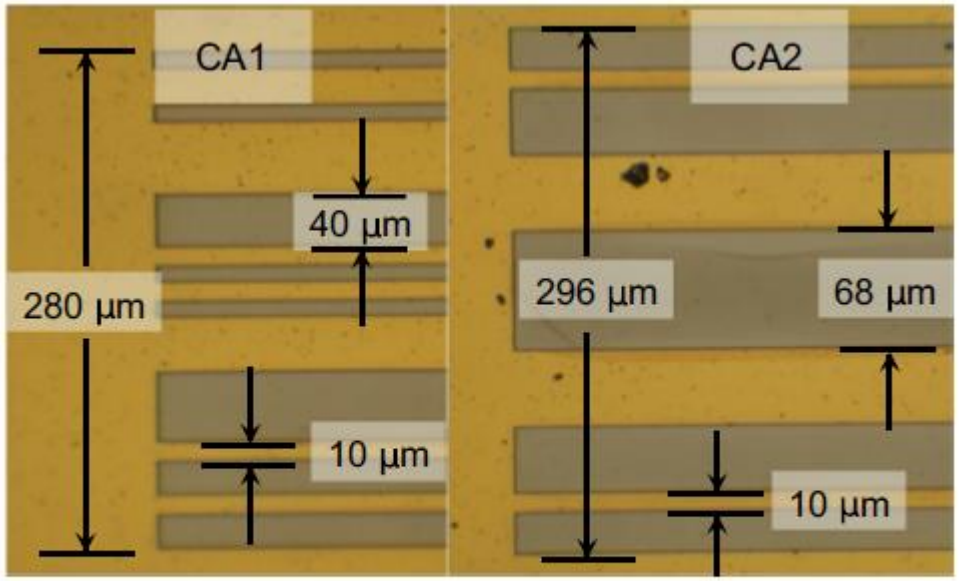

Fig. 2. Photographs of portions of CESR-TA xBSM coded aperture optical elements CA1 (left) and CA2 (right). Dark strips indicate transmission slits, while lighter areas represent the gold coating. The imperfections (black spots) are remnants of etching resist with thickness ~0.01 μm, which are essentially transparent to x-rays.

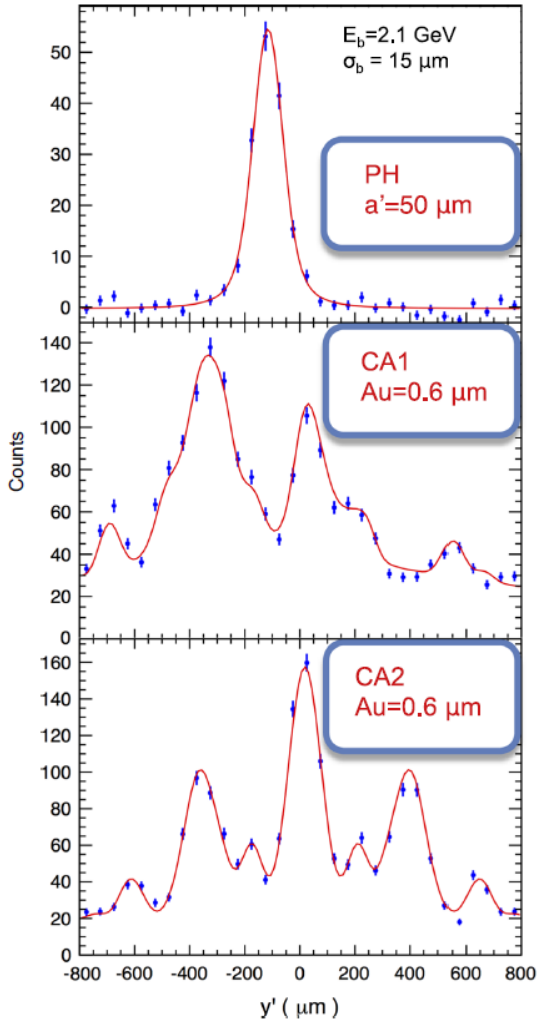

Fig. 4. Detector images (points with error bars) taken at E_b=2.1 GeV using the PH (top), CA1 (middle), and CA2 (bottom) optical elements. The smooth curves show the best fits, which in all cases have $\sigma_b \approx 15$ μm.

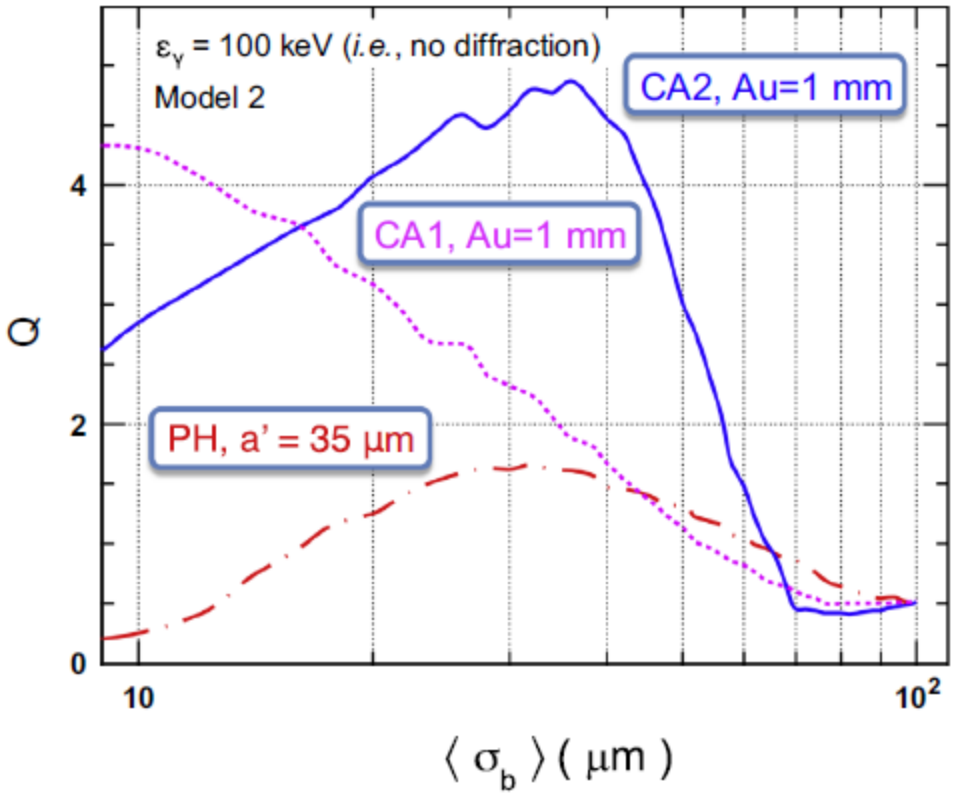

Fig. 12. Predicted figure of merit for each of three optical elements at CESR-TA in the non-diffractive, thick-masking limit.

CA2 design philosophy: intentionally optimize slit widths to enhance diffraction peaks over detectable spectrum to create sharper edges in PSF.

J.P. Alexander et al., Nuclear Instruments and Methods in Physics Research A767(2014) 467–474

SuperKEKB X-ray monitor

SuperKEKB is a 2-ring collider.
X-ray beam lines installed in both Low Energy Ring (LER) and High Energy Ring (HER).

X-ray beam line at LER

Similar line also at HER

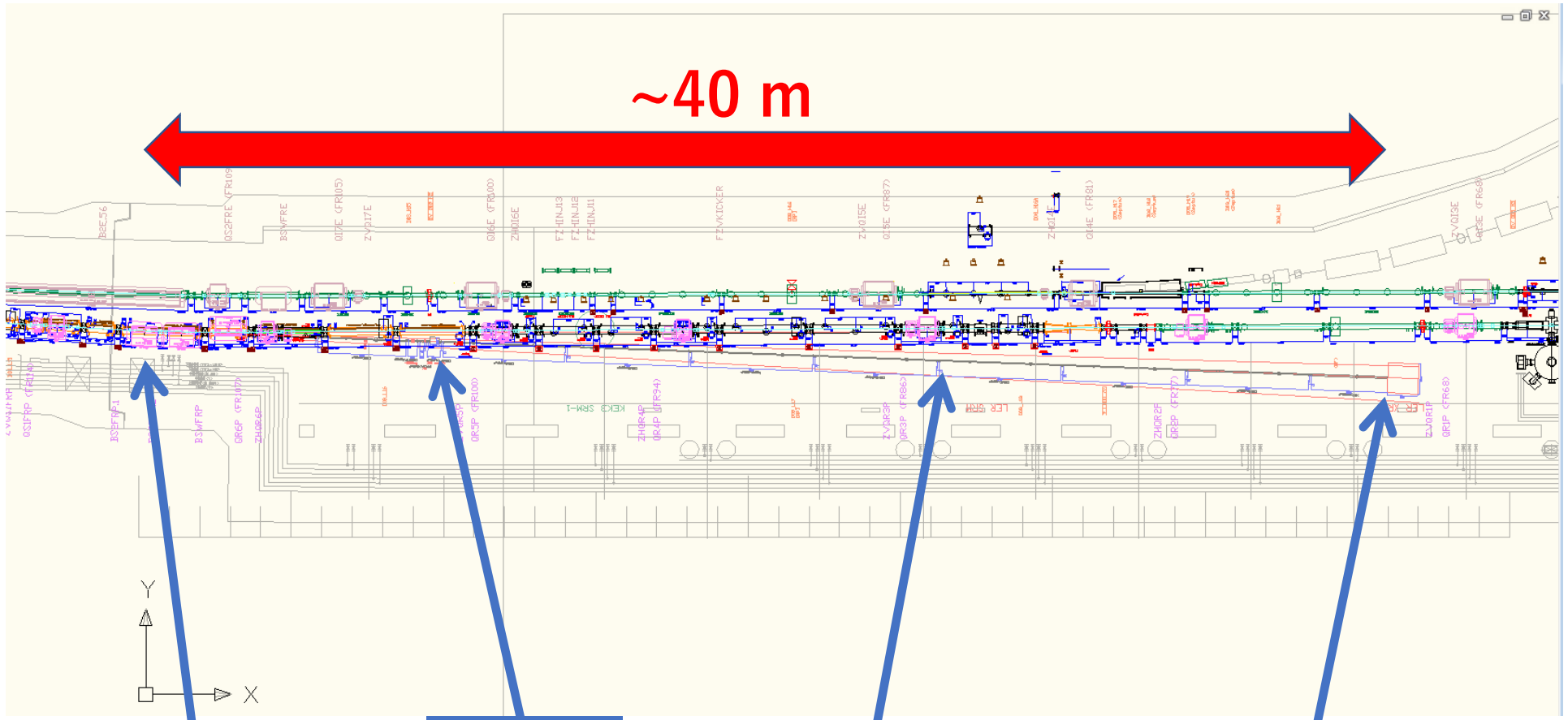

SuperKEKB X-ray beam profile Monitor

Mask patterns

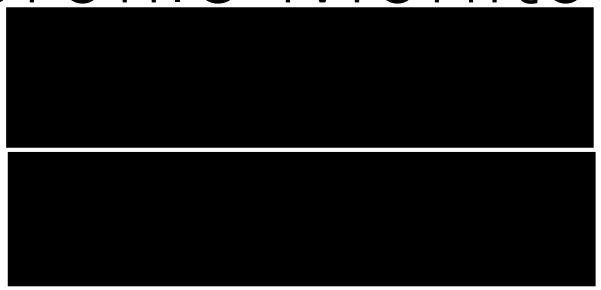

Single slit, 33 μm wide

Note: All three mask patterns based on units of optimal slit width for minimizing PSF.

Single slit: 33 μm

Multi-slit: 33 μm slits at varying spacings

URA: Slits and spacings are all multiples of 33 μm

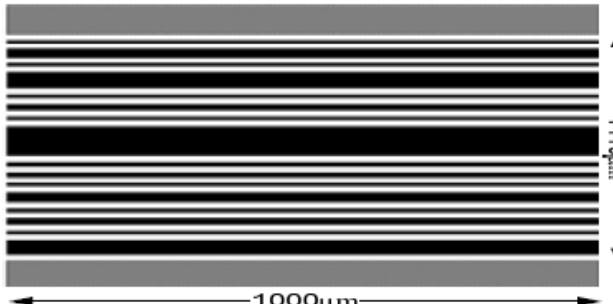

Multi-slit mask (E. Mulyani)

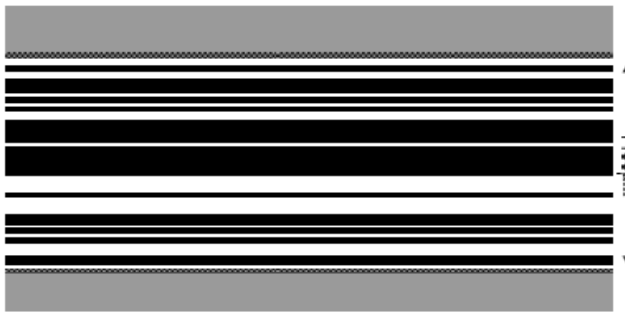

URA mask (E. E. Fenimore, T. M. Cannon, Appl. Optics, Vol 17, No.3, 337 (1978).

Calculated images for different beam sizes

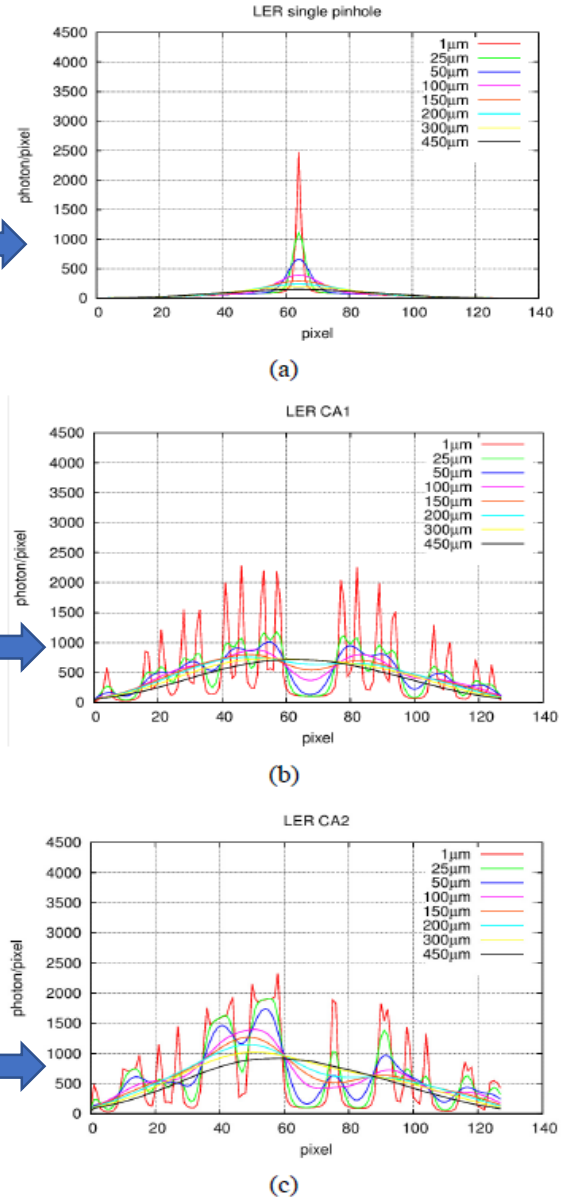

Figure 6: Simulated detector images showing the number of photons/pixel for 1 mA bunches for different beam sizes at LER: (a) single pinhole; (b) CA1; (c) CA2.

Single-shot statistical resolutions expected

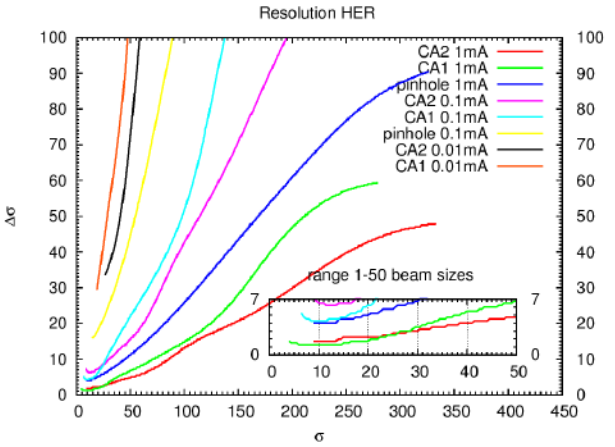

Figure 7: Vertical beam size resolutions at HER for various bunch currents (1 mA, 0.1 mA and 0.01 mA) and optical elements (single pinhole, CA1 and CA2).

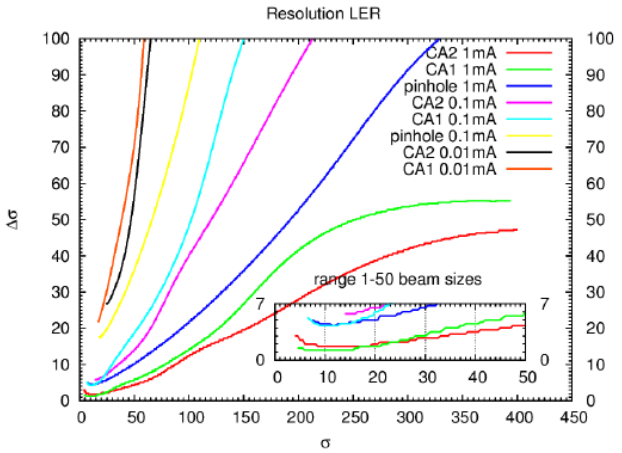

Figure 8: Vertical beam size resolutions at LER for various bunch currents (1 mA, 0.1 mA and 0.01 mA) and optical elements (single pinhole, CA1 and CA2).

E. Mulyani and J. Flanagan, TUPB025, Proc. IBIC2015, Melbourne

SuperKEKB X-ray Monitor: Hardware

X-ray beam line under construction at LER

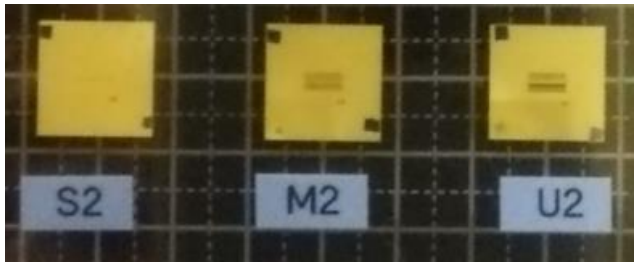

Masks: ~20 μm Au on 600 μm CVD diamond substrate

Water-cooled mask holder

US-Japan Collaboration (U. Hawaii, SLAC, Cornell U.)

High-speed readout electronics for the X-ray monitor, being developed by U of Hawaii.

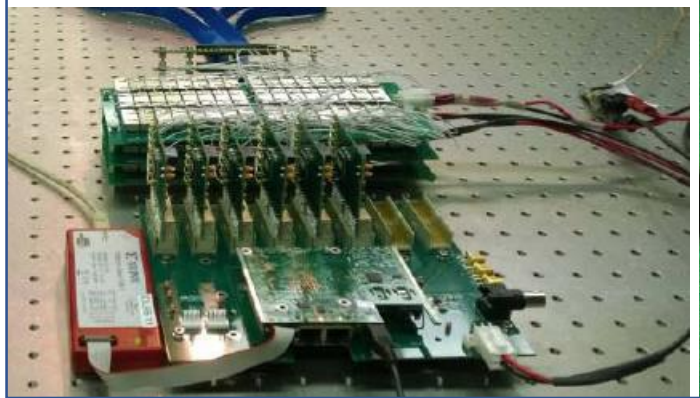

Deep Si pixel detector and spectrometer chips for the X-ray monitor, being developed at SLAC.

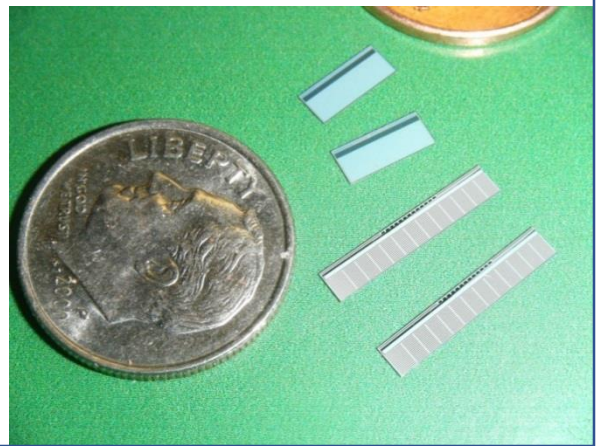

Scintillator read-out system for Phase I of SuperKEKB commissioning (Spring 2016)

E. Mulyani and J.W. Flanagan, **"CALIBRATION OF X-RAY MONITOR DURING THE PHASE I OF SuperKEKB COMMISSIONING"** Proceedings of IBIC2016, Barcelona, Spain (2016) 524.

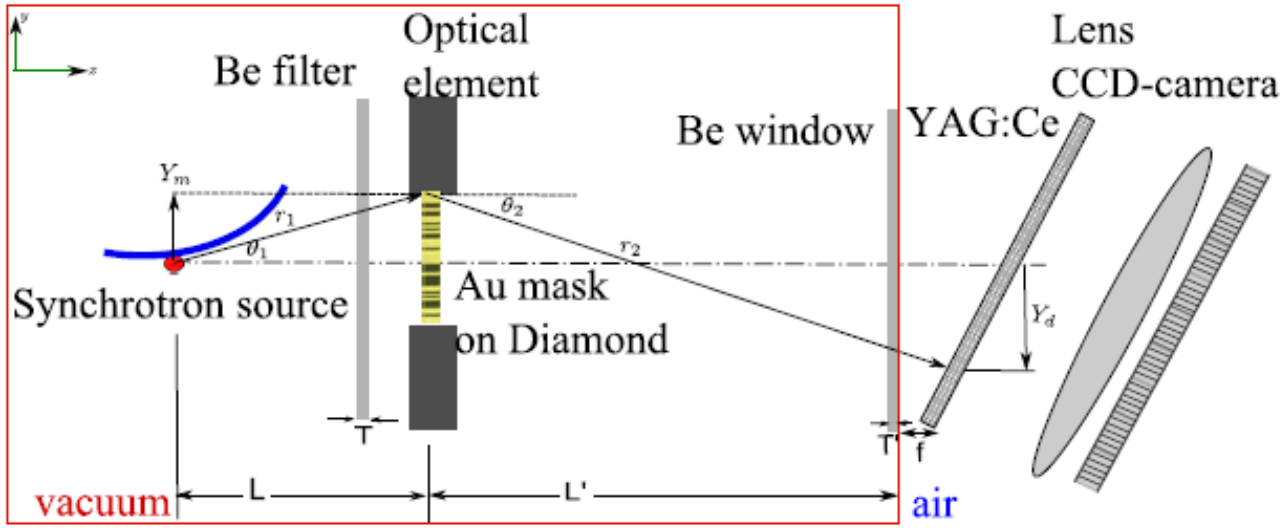

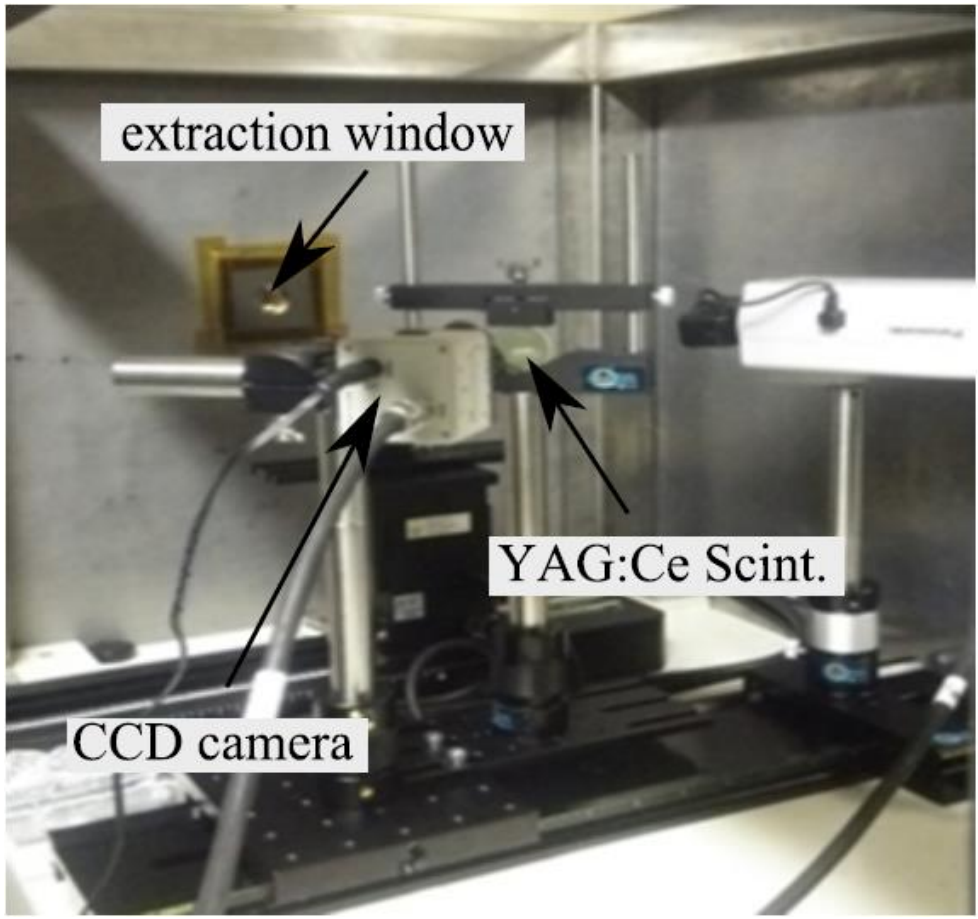

Figure 8: Schematic of XRM Beam Line. The beam passes through the Be filter, optical elements and Be window, and is then deposited in the 141 μm thick YAG scintillator.

SuperKEKB X-ray Monitor: control room display panel

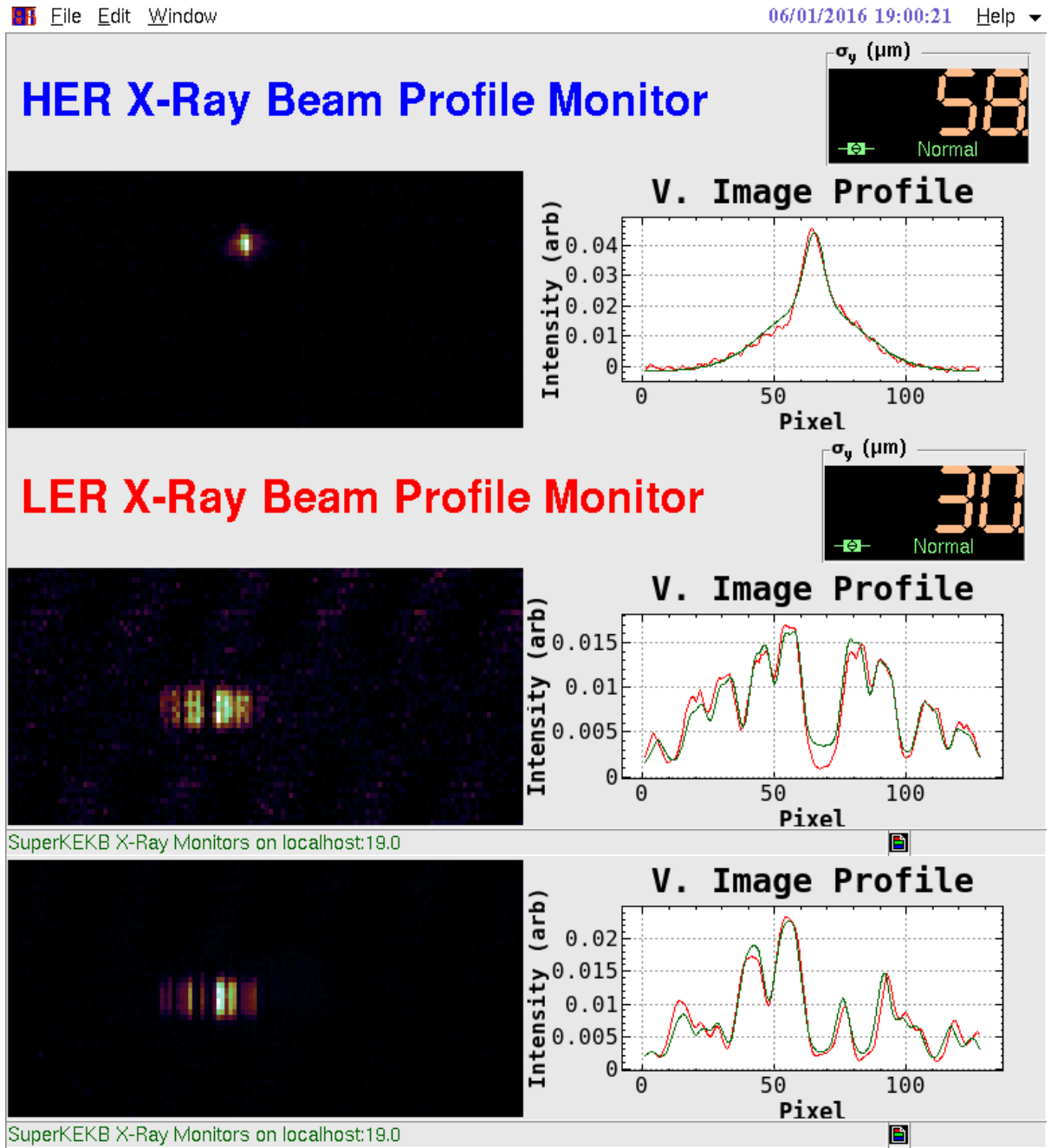

Single-slit mask

Multi-slit mask

URA mask

SuperKEKB XRM: Status

- HER and LER beam lines commissioned, and taking data with scintillators.
- Template fits implemented for taking data with single-slit, multi-slit and URA masks.
- Calibration studies undertaken:
  - Source-point measurement
  - Overall magnification studies
    - Emittance Knob studies
    - Mask movement studies
    - Source-point movement studies
    - Changing beta function at source point (HER)
  - Light-level dependence (HER)
- Beam studies undertaken
  - Emittance measurements at LER and HER,
  - Electron cloud (LER) and current-dependence (HER)

SuperKEKB XRM: e-cloud blow-up study (LER)

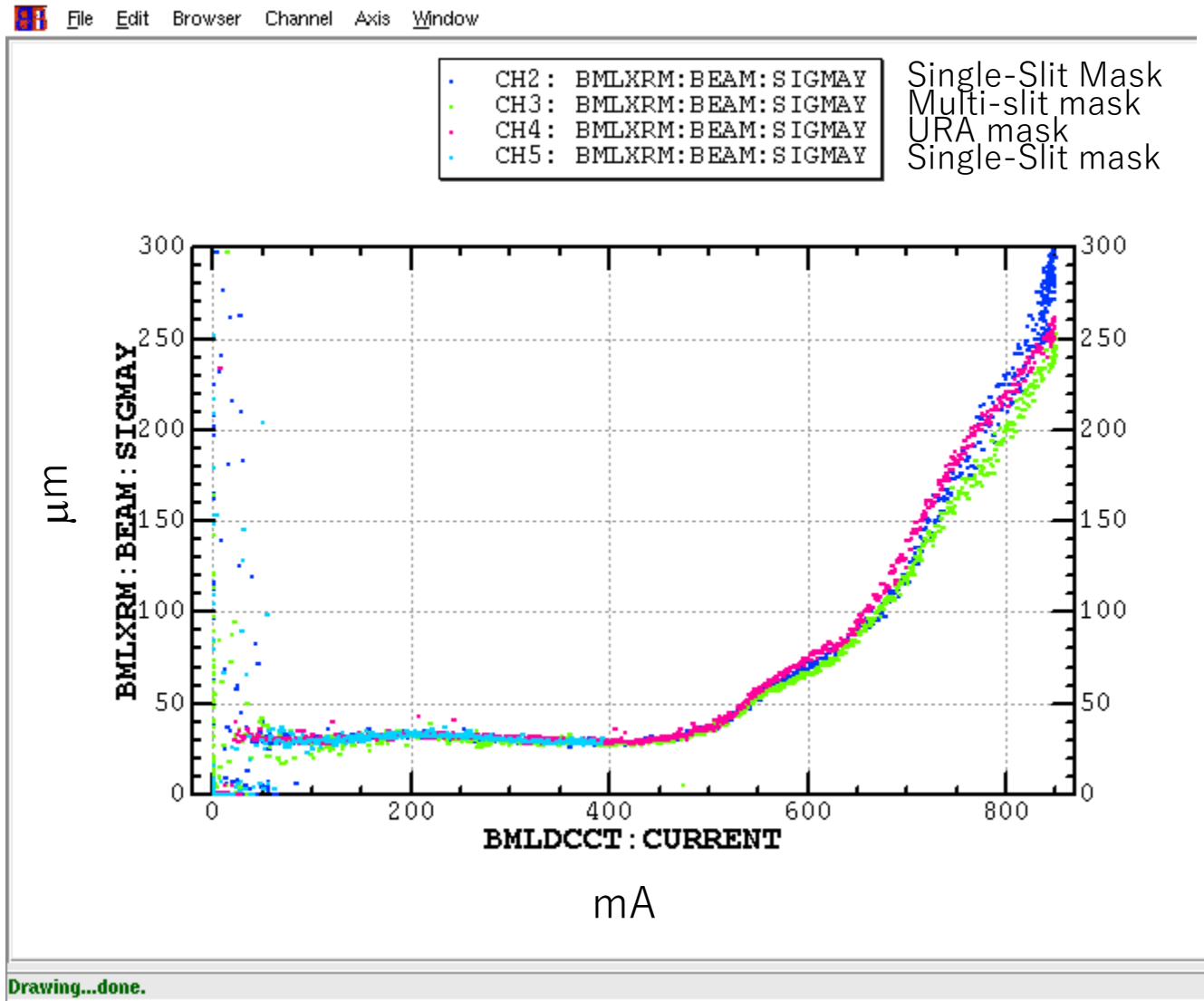

Very good fill-to-fill repeatability

Very good agreement between different masks, especially below 150 μm.

Experience at SuperKEKB

- Issues identified:
  - Suspect excessive scattering at Be filter
    - Replaced Be filters with thinner ones for Phase II
  - Excessive ionization in air path
    - Filled detector box with helium for Phase II
  - Will replace cameras with higher-resolution versions later this year.
  - Most importantly, will start commissioning high-speed single-shot measurement system later this year.

Visible x-ray path in air (LER, 100 mA):

SuperKEKB Prospects

- Recall that I mentioned that template fitting works when basic source distribution is known, and characterized by a small number of parameters.
- For instability studies, such as electron-cloud-induced head-tail instabilities, the source distribution can become quite perverse. In fact, becoming non-Gaussian can itself be a diagnostic for the onset of certain instabilities. So it would be nice to be able to reconstruct the image of the beam.

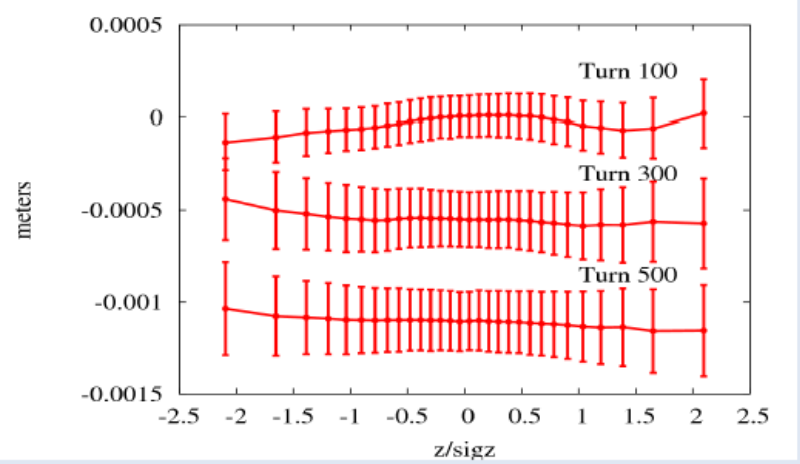

E-cloud induced head-tail motion simulation, adapted from E. Benedetto *et al*, PAC07, 4033 (2007)

- Which brings us back to the direct deconvolution reconstruction methods, which are being studied by E. Mulyani for use at SuperKEKB.
  - This would be especially useful for single-shot measurements, which are not averaged over many bunches and turns.
  - Direct deconvoution is much faster than template fitting, if potentially less accurate.
    - 2500 bunches * thousands of turns/bunch = a lot of data!
  - Look for results to be released later this year.

Summary

- Coded aperture techniques have been tested for beam-size measurement at Diamond Light Source, CesrTA, and SuperKEKB.
  - Using both URA and other mask patterns
- CA forms the primary beam size measurement system at SuperKEKB.
- Template fitting methods for measuring the beam size have been well demonstrated.
- Direct deconvolution is being tested for faster reconstruction at SuperKEKB.

Spares

URA design principles

Modified URA Mask, Anti-mask, and Cross-correlation

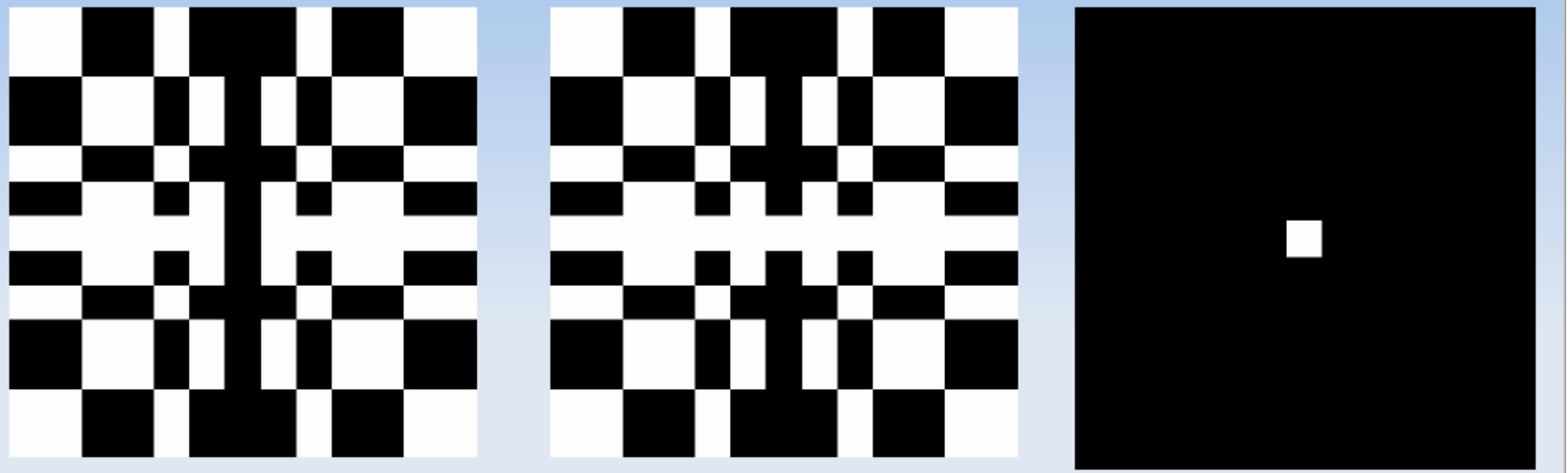

- Image is encoded using mask and decoded using anti-mask, where cross-correlation between mask and anti-mask is delta function.
- Pixel transparency determined by Jacobi function:
  - Is (pixel index)%DIM == (i*i)%DIM for any 1<i<DIM?
    - Yes/No->Open/Closed.
    - 2-D case based on inverse XOR of both indices.
- Note: Fresnel zone plates can in principle also be used as coded apertures. (Barrett, H.H., Horrigan, F.A.: 1973, Appl. Opt., 12, 2686)